Multi-Subnet Wireless Sensing Feedback for Decentralized H_2 Control with Information Overlapping

Yang Wang, Kincho H. Law, Chin-Hsiung Loh, Shieh-Kung Huang, Kung-Chun Lu, and Pei-Yang Lin

***Abstract*— This paper studies a time-delayed decentralized structural control strategy that aims to minimize the H_2 norm of the closed-loop system. In a decentralized control system, control decisions are made based on data acquired from sensors located in the vicinity of a control device. Due to the non-convexity nature of the optimization problem caused by a decentralized architecture, controller design for decentralized systems remains a major challenge. In this work, a homotopy method is employed to gradually transform a centralized controller into multiple decentralized controllers. Linear matrix inequality (LMI) constraints are adopted in the homotopic transformation to ensure closed-loop control performance. In addition, multiple decentralized control architectures are implemented with a network of wireless sensing and control nodes. The sensor network allows simultaneous operation of multiple wireless subnets. Both the theoretical development and system implementation support the information overlapping between decentralized subnets. For validation, the wireless sensing and control system is installed on a six-story laboratory steel structure controlled by magnetorheological (MR) dampers. Shake-table experiments are conducted to demonstrate the performance of the wireless decentralized control strategies.**

I. Introduction

A feedback structural control system contains networked sensors, controller, and control devices that are deployed in a structure, such as buildings or bridges (Soong 1990). When dynamic excitation (e.g. earthquake or typhoon) occurs, structural vibrations are recorded by the sensors. In real time, the sensor data is collected by the controller and processed for control decisions. The command signals are then immediately dispatched from the controller to the control devices, so that excessive dynamic responses of the structure can be mitigated.

A traditional structural control system has one centralized controller, which is responsible for acquiring data from all sensors and making control decisions for all control devices. For deployment on a large scale structure, such centralized architecture may result in very high installation cost, cause significant communication and computation latency, and pose the risk of bottleneck failure. To mitigate some of the difficulties with centralized feedback control systems, decentralized control strategies can be explored (Sandell, *et al.* 1978; Siljak 1991). In a decentralized control system, distributed controllers are designed to make control decisions using only the data from neighboring sensors, and to command control devices in the vicinity area. The feedback latency can be reduced, and the centralized bottleneck can be removed. In addition, using state-of-the-art wireless communication and embedded computing technologies, the instrumentation cost of the decentralized control network can be significantly lower (Wang and Law 2007).

Towards decentralized structural control, Wang *et al.* (2007) described a decentralized static output feedback control strategy that is based upon the linear quadratic regulator (LQR) criteria. Sparsity shape constraints upon the gain matrices are employed to represent decentralized feedback patterns; iterative gradient searching is adopted for computing decentralized gain matrices that optimize the control performance over the entire structure. Lu, *et al.* (2008) studied the performance of fully decentralized sliding mode control algorithms; the algorithms require only the stroke velocity and displacement of a control device to make the control decision. For structural systems that are instrumented with collocated rate sensors and actuators, Hiramoto and Grigoriadis (2008) explored decentralized static feedback controller design in continuous-time domain.

This paper presents a time-delayed decentralized structural control strategy that aims to minimize the H_2 norm of the closed-loop system. Centralized H_2 controller design for structural control has been studied by many researchers, through both laboratory experiments and numerical simulations (Dyke, *et al.* 1996; Johnson, *et al.* 1998; Yang, *et al.* 2003). Their studies have shown the effectiveness of centralized H_2 control for civil structures. In contrast, this paper focuses on the time-delayed decentralized H_2 controller design. The decentralized controller design employs a homotopy method that gradually transforms a centralized controller into multiple decentralized controllers. Linear matrix inequality constraints are included in the homotopic transformation to ensure optimal control performance. The approach is adapted from the homotopy method described by Zhai, *et al.* (2001), where the method was originally developed for designing decentralized H_∞ controllers in continuous-time domain.

With regard to the implementation of the decentralized

Manuscript received September 22, 2010. This work was partially supported by NSF, Grant Number CMMI-0824977, awarded to Prof. Kincho H. Law of Stanford University.

Y. Wang is at the School of Civil and Environmental Engineering, Georgia Institute of Technology, Atlanta, GA 30332, USA (phone: 1-404-894-1851; fax: 1-404-894-2278; e-mail: yang.wang@ce.gatech.edu).

K. H. Law is at the Department of Civil and Environmental Engineering, Stanford University, Stanford, CA 94305, USA.

C.-H. Loh, K.-C. Lu, and P.-Y. Lin are at the Department of Civil Engineering, National Taiwan University, Taipei 106, Taiwan.

S.-K. Huang is at the National Center for Research on Earthquake Engineering, Taipei 106, Taiwan.

control system, this study explores wireless communication for the sensing and control network. In order to allow multiple decentralized controllers to simultaneously obtain real-time data from neighborhood sensors over a wireless network, multiple subnets that operate on different wireless communication channels are deployed to minimize interference among the subnets. Besides handling real-time communication, the microprocessor of each wireless sensing and control unit also needs to coordinate the sensing and actuation tasks (such as sensor interrogation, embedded computing, and control signal generation) with accurate timing. This paper presents the implementation of a real-time wireless feedback structural control system with multi-channel low-latency communication, utilizing the Narada wireless sensing and control unit designed by Swartz and Lynch (Swartz, *et al.* 2005; Swartz and Lynch 2009). Different decentralized control architectures are implemented with a network of wireless sensing and control units instrumented on a six-story steel frame structure. Information overlapping between adjacent subnets is achieved through wireless units dedicated for relaying data. Semi-active magnetorheological dampers are installed on the structure as control devices. Shake table experiments have been conducted to examine the performance of different decentralized control strategies.

The paper is organized as follows. First, the formulation for decentralized H_2 controller design is introduced. The experimental setup of the six-story steel frame structure instrumented with wireless sensing and control system is then described. Details are provided on the information-overlapping control architectures achieved by simultaneous real-time sensing feedback using multiple wireless subnets. Experimental and simulation results are presented to evaluate the effectiveness of the decentralized H_2 control strategies.

II. Basic Formulation

For a structural model with n degrees-of-freedom (DOF) and instrumented with n_u control devices, the structural system and a system describing time-delay and sensor noise effect can be cascaded into an open-loop system in discrete-time domain (Wang 2010):

$$\begin{cases} \mathbf{x}[k+1] = \mathbf{A}\mathbf{x}[k] + \mathbf{B}_1\mathbf{w}[k] + \mathbf{B}_2\mathbf{u}[k] \\ \mathbf{z}[k] = \mathbf{C}_1\mathbf{x}[k] + \mathbf{D}_{11}\mathbf{w}[k] + \mathbf{D}_{12}\mathbf{u}[k] \\ \mathbf{y}[k] = \mathbf{C}_2\mathbf{x}[k] + \mathbf{D}_{21}\mathbf{w}[k] + \mathbf{D}_{22}\mathbf{u}[k] \end{cases} \quad (1)$$

The system input $\mathbf{w} = [\mathbf{w}_1{}^{\mathrm{T}}\ \mathbf{w}_2{}^{\mathrm{T}}]^{\mathrm{T}} \in \mathbb{R}^{n_w \times 1}$ contains both external excitation $\mathbf{w}_1$ and sensor noise $\mathbf{w}_2$; $\mathbf{u} \in \mathbb{R}^{n_u \times 1}$ denotes the control force vector; the open-loop state vector, $\mathbf{x} \in \mathbb{R}^{n_{OL} \times 1}$, contains $\mathbf{x}_S \in \mathbb{R}^{2n \times 1}$, the state vector of the structural system, and $\mathbf{x}_{TD} \in \mathbb{R}^{n_{TD} \times 1}$, the state vector of the time-delay and sensor noise system. For a lumped mass structural model with n stories, the state vector of the structural dynamics, $\mathbf{x}_S$, consists of the relative displacement q_i and relative velocity $\dot{q}_i$ (with respect to the ground) for each floor i, $i = 1, \ldots n$.

$$\mathbf{x}_S = [q_1 \ \ \dot{q}_1 \ \ q_2 \ \ \dot{q}_2 \ \ \ldots \ q_n \ \ \dot{q}_n]^{\mathrm{T}} \quad (2)$$

The matrices $\mathbf{A} \in \mathbb{R}^{n_{OL} \times n_{OL}}$, $\mathbf{B}_1 \in \mathbb{R}^{n_{OL} \times n_w}$, and $\mathbf{B}_2 \in \mathbb{R}^{n_{OL} \times n_u}$ are, respectively, the discrete-time dynamics, excitation influence, and control influence matrices. The vector $\mathbf{z} \in \mathbb{R}^{n_z \times 1}$ represents the response output (to be controlled through the feedback loop), and $\mathbf{y} \in \mathbb{R}^{n_y \times 1}$ represents the time-delayed and noisy sensor signals. Correspondingly, the matrices $\mathbf{C}_1$, $\mathbf{D}_{11}$, and $\mathbf{D}_{12}$ are termed the output parameter matrices, and the matrices $\mathbf{C}_2$, $\mathbf{D}_{21}$, and $\mathbf{D}_{22}$ are the measurement parameter matrices. Time delay of one sampling period ΔT is assumed for the sensor measurement signal (e.g. due to computational and/or communication latency). The formulation can easily be extended to model multiple time delay steps, as well as different time delays for different sensors. Furthermore, the formulation can represent fully decentralized control architecture, as well as information overlapping in a partially decentralized control architecture. Detailed description about the formulation can be found in Wang (2010).

Fig. 1 summarizes the components of the control system. As shown in the figure, the open-loop system formulated in Eq. (1) contains the structural system and the system describing time delay, noise, and possible signal repeating. Output of the structural system, i.e. sensor measurement, is an input to the time-delay system. For the overall open-loop system, the inputs include the excitation $\mathbf{w}_1[k]$, the sensor noises $\mathbf{w}_2[k]$, and the control forces $\mathbf{u}[k]$; outputs of the open-loop system include the structural response $\mathbf{z}[k]$ and the feedback signals $\mathbf{y}[k]$. To complete the feedback control loop, the controller system takes the signal $\mathbf{y}[k]$ as input and generates the desired (optimal) control force vector $\mathbf{u}[k]$ according to the following state-space equations:

$$\begin{cases} \mathbf{x}_G[k+1] = \mathbf{A}_G\mathbf{x}_G[k] + \mathbf{B}_G\mathbf{y}[k] \\ \mathbf{u}[k] = \mathbf{C}_G\mathbf{x}_G[k] + \mathbf{D}_G\mathbf{y}[k] \end{cases} \quad (3)$$

where $\mathbf{A}_G$, $\mathbf{B}_G$, $\mathbf{C}_G$ and $\mathbf{D}_G$ are the parametric matrices of the controller to be computed and, for convenience, are often collectively denoted by a controller matrix $\mathbf{G} \in \mathbb{R}^{(n_G+n_u)\times(n_G+n_y)}$ as:

$$\mathbf{G} = \begin{bmatrix} \mathbf{A}_G & \mathbf{B}_G \\ \mathbf{C}_G & \mathbf{D}_G \end{bmatrix} \quad (4)$$

In this study, we assume the controller and the open-loop system have the same number of state variables.

III. Decentralized H_2 Controller Design

For decentralized control design, the feedback signals $\mathbf{y}[k]$

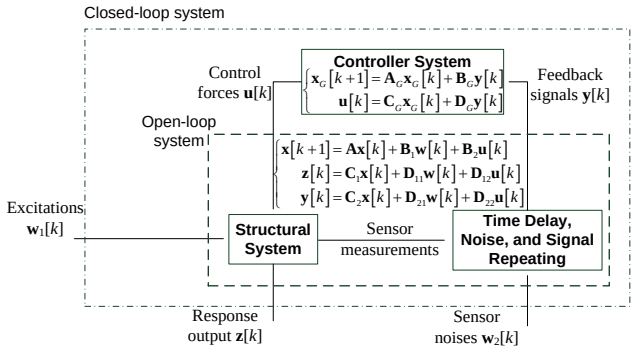

Fig. 1. Diagram of the closed-loop control system.

and the control forces $\mathbf{u}[k]$ are divided into N groups. For determining each group of control force, only one group of corresponding feedback signals is needed. To achieve this decentralized feedback pattern, the controller matrices can be specified to be block diagonal:

$$\mathbf{A}_G = diag\left(\mathbf{A}_{G_I}, \mathbf{A}_{G_{II}}, \cdots, \mathbf{A}_{G_N}\right) \tag{5a}$$

$$\mathbf{B}_G = diag\left(\mathbf{B}_{G_I}, \mathbf{B}_{G_{II}}, \cdots, \mathbf{B}_{G_N}\right) \tag{5b}$$

$$\mathbf{C}_G = diag\left(\mathbf{C}_{G_I}, \mathbf{C}_{G_{II}}, \cdots, \mathbf{C}_{G_N}\right) \tag{5c}$$

$$\mathbf{D}_G = diag\left(\mathbf{D}_{G_I}, \mathbf{D}_{G_{II}}, \cdots, \mathbf{D}_{G_N}\right) \tag{5d}$$

The control system in Eq. (3) is thus equivalent to a set of uncoupled decentralized controllers $\mathbf{G}_i$ ($i = I, II, \ldots, N$):

$$\mathbf{G}_i = \begin{bmatrix} \mathbf{A}_{G_i} & \mathbf{B}_{G_i} \\ \mathbf{C}_{G_i} & \mathbf{D}_{G_i} \end{bmatrix} \tag{6}$$

Each controller $\mathbf{G}_i$ requires only one group of feedback signals to determine one group of desired control forces:

$$\begin{cases} \mathbf{x}_{G_i}[k+1] = \mathbf{A}_{G_i}\mathbf{x}_{G_i}[k] + \mathbf{B}_{G_i}\mathbf{y}_i[k] \\ \mathbf{u}_i[k] = \mathbf{C}_{G_i}\mathbf{x}_{G_i}[k] + \mathbf{D}_{G_i}\mathbf{y}_i[k] \end{cases} \tag{7}$$

Assuming that the $\mathbf{D}_{22}$ matrix in the open-loop system in Eq. (1) is a zero matrix, following notations are defined:

$$\left[\begin{array}{c|c|c} \tilde{\mathbf{A}} & \tilde{\mathbf{B}}_1 & \tilde{\mathbf{B}}_2 \\ \hline \tilde{\mathbf{C}}_1 & \tilde{\mathbf{D}}_{11} & \tilde{\mathbf{D}}_{12} \\ \hline \tilde{\mathbf{C}}_2 & \tilde{\mathbf{D}}_{21} & \end{array}\right] = \left[\begin{array}{cc|c|cc} \mathbf{A} & \mathbf{0} & \mathbf{B}_1 & \mathbf{0} & \mathbf{B}_2 \\ \mathbf{0} & \mathbf{0}_{n_G} & \mathbf{0} & \mathbf{I}_{n_G} & \mathbf{0} \\ \hline \mathbf{C}_1 & \mathbf{0} & \mathbf{D}_{11} & \mathbf{0} & \mathbf{D}_{12} \\ \hline \mathbf{0} & \mathbf{I}_{n_G} & \mathbf{0} & & \\ \mathbf{C}_2 & \mathbf{0} & \mathbf{D}_{21} & & \end{array}\right] \tag{8}$$

where zero submatrices with unspecified dimensions should have compatible dimensions with neighboring submatrices. For either centralized or decentralized control, the closed-loop system can be formulated by concatenating the open-loop system in Eq. (1) with the controller system in Eq. (3):

$$\begin{cases} \mathbf{x}_{CL}[k+1] = \mathbf{A}_{CL}\mathbf{x}_{CL}[k] + \mathbf{B}_{CL}\mathbf{w}[k] \\ \mathbf{z}[k] = \mathbf{C}_{CL}\mathbf{x}_{CL}[k] + \mathbf{D}_{CL}\mathbf{w}[k] \end{cases} \tag{9}$$

where

$$\mathbf{A}_{CL} = \tilde{\mathbf{A}} + \tilde{\mathbf{B}}_2\mathbf{G}\tilde{\mathbf{C}}_2 \tag{10a}$$

$$\mathbf{B}_{CL} = \tilde{\mathbf{B}}_1 + \tilde{\mathbf{B}}_2\mathbf{G}\tilde{\mathbf{D}}_{21} \tag{10b}$$

$$\mathbf{C}_{CL} = \tilde{\mathbf{C}}_1 + \tilde{\mathbf{D}}_{12}\mathbf{G}\tilde{\mathbf{C}}_2 \tag{10c}$$

$$\mathbf{D}_{CL} = \tilde{\mathbf{D}}_{11} + \tilde{\mathbf{D}}_{12}\mathbf{G}\tilde{\mathbf{D}}_{21} \tag{10d}$$

and $\mathbf{G}$ is as defined in Eq. (4). Note that the input to the closed-loop system is $\mathbf{w}[k]$, which contains the external excitation $\mathbf{w}_1[k]$ and sensor noises $\mathbf{w}_2[k]$, while the output is the same as the structural output $\mathbf{z}[k]$ defined in Eq. (1). Using Z-transform, the dynamics of a discrete-time system can be represented by the transfer function $\mathbf{H}_{\mathbf{zw}}(z) \in \mathbb{C}^{n_z \times n_w}$ from disturbance $\mathbf{w}$ to output $\mathbf{z}$ as:

$$\mathbf{H}_{\mathbf{zw}}(z) = \mathbf{C}_{CL}\left(z\mathbf{I} - \mathbf{A}_{CL}\right)^{-1}\mathbf{B}_{CL} + \mathbf{D}_{CL} \tag{11}$$

The objective of H_2 control design is to minimize the H_2-norm of the closed-loop discrete-time system, which in the frequency domain is defined as:

$$\left\|\mathbf{H}_{\mathbf{zw}}\right\|_2 = \sqrt{\frac{\Delta T}{2\pi}\int_{-\omega_N}^{+\omega_N} \mathrm{Trace}\left\{\mathbf{H}_{\mathbf{zw}}^*\left(e^{\mathrm{j}\omega\Delta T}\right)\mathbf{H}_{\mathbf{zw}}\left(e^{\mathrm{j}\omega\Delta T}\right)\right\} d\omega} \tag{12}$$

where ω represents angular frequency, $\omega_N = \pi/\Delta T$ is the Nyquist frequency, j is the imaginary unit, $\mathbf{H}_{\mathbf{zw}}^*$ is the complex conjugate transpose of $\mathbf{H}_{\mathbf{zw}}$, and $\mathrm{Trace}\{\square\}$ denotes the trace of a square matrix. Based upon well-known equivalence between H_2 -norm criterion and matrix inequalities (Masubuchi, *et al.* 1998), it can be derived that the H_2 -norm of the closed-loop system is less than a positive number γ; if, and only if, there exist symmetric positive definite matrices $\mathbf{P}$ and $\mathbf{R}$ such that the following inequalities holds:

$$\mathbf{F}_1(\mathbf{G},\mathbf{P}) = \begin{bmatrix} \mathbf{P} & \mathbf{P}\left(\tilde{\mathbf{A}} + \tilde{\mathbf{B}}_2\mathbf{G}\tilde{\mathbf{C}}_2\right) & \mathbf{P}\left(\tilde{\mathbf{B}}_1 + \tilde{\mathbf{B}}_2\mathbf{G}\tilde{\mathbf{D}}_{21}\right) \\ * & \mathbf{P} & \mathbf{0} \\ * & * & \mathbf{I} \end{bmatrix} > 0 \tag{13a}$$

$$\mathbf{F}_2(\mathbf{G},\mathbf{P},\mathbf{R}) = \begin{bmatrix} \mathbf{R} & \tilde{\mathbf{C}}_1 + \tilde{\mathbf{D}}_{12}\mathbf{G}\tilde{\mathbf{C}}_2 & \tilde{\mathbf{D}}_{11} + \tilde{\mathbf{D}}_{12}\mathbf{G}\tilde{\mathbf{D}}_{21} \\ * & \mathbf{P} & \mathbf{0} \\ * & * & \mathbf{I} \end{bmatrix} > 0 \tag{13b}$$

$$\mathrm{Trace}(\mathbf{R}) < \gamma \tag{13c}$$

where * denotes a symmetric entry; "> 0" means that the matrix at the left side of the inequality is positive definite.

For centralized control, efficient algorithms and solvers are available for computing controller matrices that minimizes the

closed-loop H_2-norm. For a decentralized control solution, the H_2-norm criterion $\|\mathbf{H}_{zw}\|_2 < \gamma$ is satisfied only if a decentralized controller matrix **G** (with parametric structures illustrated in Eq. (5)), together with symmetric positive definite matrices **P** and **R**, can be found so that the three inequalities in Eq. (13) are satisfied. Because both **G** and **P** are unknown variables, the constraint $\mathbf{F}_1(\mathbf{G},\mathbf{P}) > 0$ has a bilinear matrix inequality (BMI) constraint (VanAntwerp and Braatz 2000); off-the-shelf algorithms or numerical packages for solving such usually non-convex problems are not available.

A heuristic homotopy method for designing continuous-time decentralized H_∞ controllers, which was described by Zhai, *et al.* (2001), is adapted for the discrete-time H_2 controller design in this study. Starting with a pre-computed centralized controller $\mathbf{G}_C$, the homotopy method gradually transforms the controller into a decentralized controller $\mathbf{G}_D$ along the following path:

$$\mathbf{G} = (1-\lambda)\mathbf{G}_C + \lambda\mathbf{G}_D, 0 \le \lambda \le 1 \tag{14}$$

where λ gradually increases from 0 to 1. For a total number of M steps assigned for the homotopy path, the increment is specified as:

$$\lambda_k = k/M, k = 0,1,...,M \tag{15}$$

At every step k along the homotopy path, the two matrix variables, $\mathbf{G}_D$ and **P**, are held constant one at a time, so that only one of them needs to be solved at each time. In this way, the BMI constraint in Eq. (13) degenerates into a linear matrix inequality (LMI) constraint that can be solved efficiently. If the homotopy transformation finishes successfully (i.e. λ reaches 1), the $\mathbf{G}_D$ computed at the final step is a decentralized controller that satisfies the norm criterion. However, it should be pointed out that since the homotopy method is heuristic in nature, non-convergence in the computation does not imply that the decentralized H_2 control problem has no solution.

IV. Shake Table Experiments

To study the performance of the decentralized H_2 structural control architecture with a wireless feedback control system, shake table experiments on a six-story laboratory structure are conducted. This section describes the experimental setup, control strategies, and test results.

A. Experimental Setup

Shake table experiments are conducted on a six-story laboratory structure recently designed, built, and improved at the National Center for Research on Earthquake Engineering (NCREE) in Taipei, Taiwan. The structure is mounted on a 5m × 5m 6-DOF shake table (see Fig. 2a). For this study, only longitudinal excitations are used. Accelerometers, velocity

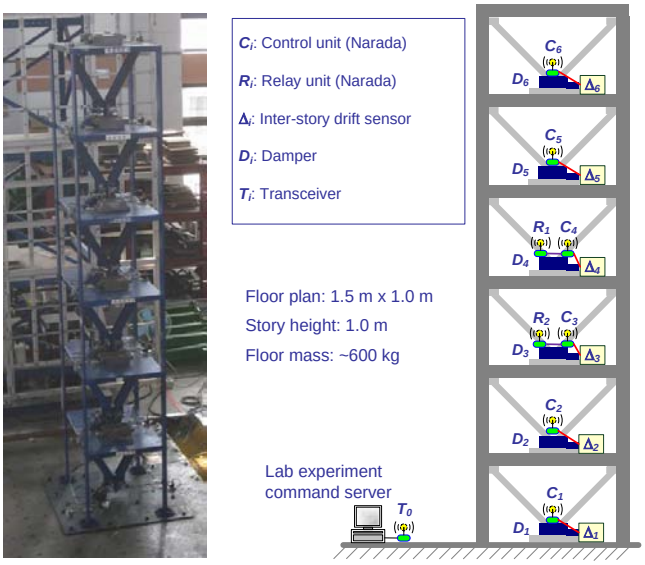

(a) (b)

Fig. 2. Six-story structure for control experiments: (a) picture of the structure on the shake table; (b) schematic of the setup.

meters, and linear variable displacement transducers (LVDTs) are instrumented on the shake table and on every floor to record the dynamic responses of the structure. The sensors are interfaced to a high-precision cabled data acquisition (DAQ) system at the NCREE facility; the cabled DAQ system is set to operate with a sampling rate of 200 Hz.

For wireless sensing and control, the prototype Narada wireless units (Swartz, *et al.* 2005) developed at the University of Michigan is employed. The wireless unit is incorporated with an onboard D/A converter for control signal generation, and a Chipcon CC2420 Zigbee transceiver for wireless communication. The basic configuration of the wireless sensing and control system for the 6-story structure is schematically shown in Fig. 2(b). A total of six wireless control units, C_1 ~ C_6, are installed in accordance with the deployment strategy. Two relay units, R_1 and R_2, are used for relaying data between different wireless channels (subnets), when needed. During the experiments, each Narada wireless unit collects inter-story drift data measured by a MTS Temposonics® C-Series magnetostrictive position sensor (Δ_1 ~ Δ_6). Each position sensor is installed between a lower floor and the bottom of a stiff V-brace connected with the upper floor.

In addition to collecting and communicating the inter-story drift data, each wireless unit sends command signal to an associated magnetorheological (MR) damper (RD-1005-3 manufactured by Lord Corporation). The damper on each floor (D_1 ~ D_6) is connected to the upper floor through the V-brace (Fig. 2a). Each damper can provide a maximum damping force over 2kN. The damping properties can be changed by the command voltage signal (ranging from 0 to 0.8V) through an input current source, which determines the electric current of the electromagnetic coil in the MR damper. The current then generates a variable magnetic field that sets

the viscous damping properties of the MR damper. Calibration tests are first conducted on the MR dampers before mounting them onto the structure and a modified Bouc-Wen force-displacement model is developed for the damper (Lu, *et al.* 2008). In the feedback control tests, updating the hysteresis model parameters for the MR dampers is an integral element of the control procedure, which is embedded in the wireless units for calculating command voltages for the dampers.

B. Control Strategies

Following the experimental setup, the time-delayed noisy sensor signals $\mathbf{y}[k]$ in Eq. (1) is defined as the inter-story drifts between every two neighboring floors, which are measured by the magnetostrictive position sensors and collected by the wireless units. The output vector $\mathbf{z}[k]$ in Eq. (1) is defined to contain both the structural response and control effort:

$$\mathbf{z} = \begin{Bmatrix} \mathbf{z}_1 \\ \mathbf{z}_2 \end{Bmatrix} \tag{16}$$

where sub-vector $\mathbf{z}_1$ contains entries related to the inter-story drift response at all stories, and sub-vector $\mathbf{z}_2$ contains entries related to control forces. By minimizing the H_2-norm of the closed-loop system, the controller design process is essentially minimizing the "amplification effect" from the input $\mathbf{w}$ to the output $\mathbf{z}$ (Eq. (9)). The relative weighting between the structural response and the control effort is reflected by the magnitudes of $\mathbf{z}_1$ and $\mathbf{z}_2$.

Four decentralized/centralized feedback control architectures are adopted in the experiments (Fig. 3). The degrees of centralization (DC) of different architectures reflect the different communication network configurations, with each wireless channel representing one communication subnet. The wireless units assigned to a subnet are allowed to access the wireless sensor data within that subnet. For case DC1, each wireless unit only utilizes the inter-story drift between two neighboring floors for control decisions; therefore, no wireless communication is required. For case DC2, each wireless channel covers three stories and a total of two wireless channels (subnets) are in simultaneous operation; no overlapping exists between the two channels. For case DC3, each wireless channel covers four stories and the two wireless channels overlap at the 3rd and 4th stories. Relay unit R_1 operates in Channel-1, and is connected with control unit C_4 though a short data wire on the same floor; similarly, Relay unit R_2 operates in Channel-2, and is connected with control unit C_3 on the same floor (as in Fig. 2b). In Fig. 3, the dash-dot lines for the DC3 schematic represent the additional information links enabled by the two relay units. As a result, case DC3 represents a decentralized architecture with information overlapping. For case DC4, one wireless channel (subnet) is shared by all six wireless units, which is equivalent to a centralized feedback pattern.

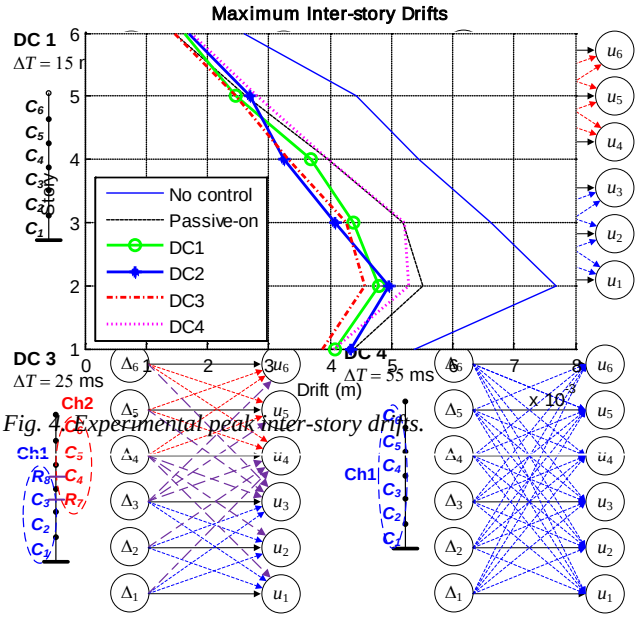

Fig. 4. Experimental peak inter-story drifts.

Fig. 3. Multiple feedback control architectures and the associated sampling time step lengths.

The control sampling time step for each control architecture is determined by the time required for wireless communication and embedded computation. The computational procedures performed by a wireless unit include updating the damper hysteresis model, calculating the desired control force for the MR damper, and determining appropriate command voltage signal for the damper. In this study, the computational time constitutes the dominant part of the feedback time delay, and the time delay is approximated as one sampling time step ΔT (in accordance with the formulation in §II). Due to different requirement on communication and computation, each control architecture can have different length of sampling time step ΔT, which is shown in Fig. 3. Because case DC1 requires minimum amount of computing, its 15ms time step (i.e. time delay) is the smallest. Cases DC2 and DC3 require more communication and computing, thus, both cases have a time step of 25ms. Due to the largest amount of communication and computation required by the centralized pattern, case DC4 has the longest time step of 55ms.

C. Experimental and Simulation Results

The 1940 El Centro NS (Imperial Valley Irrigation District Station) earthquake excitation with the peak ground acceleration (PGA) scaled to 1m/s^2 is employed in this study. Fig. 4 shows the peak inter-story drifts for different control architectures during the ground excitation, as well as the peak drifts of the uncontrolled structure (with dampers disconnected) and a passive-on control case (where the damper command voltages are all fixed to the maximum value 0.8V). Among all the passive and feedback control cases, the feedback control case DC3 achieves the most uniform peak inter-story drifts among the six stories. In addition, the three

decentralized feedback control cases generally outperform the centralized case DC4 and the passive-on case, in terms of achieving uniformly less peak drifts.

Besides the experiments, numerical simulations are conducted for different control architectures using the same scaled El Centro ground excitation. Fig. 5 shows the simulated peak inter-story drifts of the four control cases, when ideal actuators (capable of generating any desired forces) are adopted. Among all control cases, the simulation results indicate that feedback control case DC3 achieves the most uniform peak inter-story drifts among the six stories. Same as the experiments, the simulations with ideal actuation verifies that the decentralized control architecture with information overlapping can outperform other cases in terms of uniformly reducing peak inter-story drifts.

V. Summary and Discussion

This paper presents some preliminary results exploring decentralized H_2 structural control using multi-subnet wireless sensing feedback. Both the simulation and the experimental results demonstrate that the decentralized control architectures, particularly with information overlapping, achieve satisfactory control performance.

Acknowledgment

The authors appreciate the help with the wireless sensing units from Prof. J. P. Lynch and Dr. A. Zimmerman of the University of Michigan, as well as Prof. R. A. Swartz of Michigan Technological University. Any opinions, findings and conclusions expressed in this paper are those of the authors and do not necessarily reflect the views of their collaborators and sponsors.

References

[1] Dyke, S.J., Spencer, B.F., Jr., Quast, P., D. C. Kaspari, J. and Sain, M.K. (1996). "Implementation of an active mass driver using acceleration feedback control," *Computer-Aided Civil and Infrastructure Engineering*, 11(5): 305-323.

[2] Hiramoto, K. and Grigoriadis, K. (2008). "Upper bound H_∞ and H_2 control for collocated structural systems," *Structural Control and Health Monitoring*, 16(4): 425 - 440.

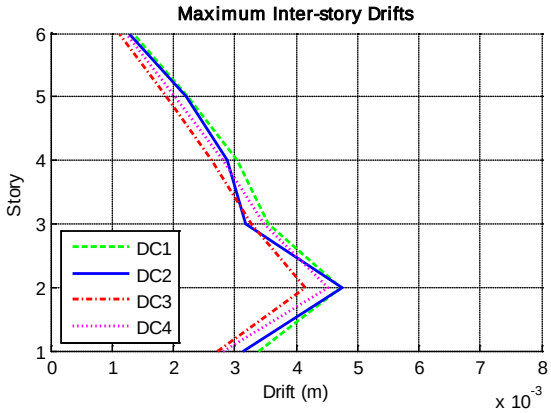

Fig. 5. Simulated peak inter-story drifts (with ideal actuators).

[3] Johnson, E.A., Voulgaris, P.G. and Bergman, L.A. (1998). "Multiobjective optimal structural control of the Notre Dame building model benchmark," *Earthquake Engineering & Structural Dynamics*, 27(11): 1165-1187.

[4] Lu, K.-C., Loh, C.-H., Yang, J.N. and Lin, P.-Y. (2008). "Decentralized sliding mode control of a building using MR dampers," *Smart Materials and Structures*, 17(5): 055006.

[5] Masubuchi, I., Ohara, A. and Suda, N. (1998). "LMI-based controller synthesis: A unified formulation and solution," *International Journal of Robust and Nonlinear Control*, 8(8): 669-686.

[6] Sandell, N., Jr., Varaiya, P., Athans, M. and Safonov, M. (1978). "Survey of decentralized control methods for large scale systems," *Automatic Control, IEEE Transactions on*, 23(2): 108-128.

[7] Siljak, D.D. (1991). *Decentralized Control of Complex Systems*, Academic Press, Boston.

[8] Soong, T.T. (1990). *Active Structural Control: Theory and Practice*, Wiley, Harlow, Essex, England.

[9] Swartz, R.A., Jung, D., Lynch, J.P., Wang, Y., Shi, D. and Flynn, M.P. (2005). "Design of a wireless sensor for scalable distributed in-network computation in a structural health monitoring system," *Proceedings of the 5th International Workshop on Structural Health Monitoring*, Stanford, CA, September 12 - 14, 2005.

[10] Swartz, R.A. and Lynch, J.P. (2009). "Strategic network utilization in a wireless structural control system for seismically excited structures," *Journal of Structural Engineering*, 135(5): 597-608.

[11] VanAntwerp, J.G. and Braatz, R.D. (2000). "A tutorial on linear and bilinear matrix inequalities," *Journal of Process Control*, 10(4): 363-385.

[12] Wang, Y., Swartz, R.A., Lynch, J.P., Law, K.H., Lu, K.-C. and Loh, C.-H. (2007). "Decentralized civil structural control using real-time wireless sensing and embedded computing," *Smart Structures and Systems*, 3(3): 321-340.

[13] Wang, Y. and Law, K.H. (2007). *Wireless Sensing and Decentralized Control for Civil Structures: Theory and Implementation*. John A. Blume Earthquake Eng. Ctr., Stanford University, Stanford, CA.

[14] Wang, Y. (2010). "Time-delayed dynamic output feedback H_∞ controller design for civil structures: a decentralized approach through homotopic transformation," *Structural Control and Health Monitoring*, http://dx.doi.org/10.1002/stc.344: in print.

[15] Yang, J.N., Lin, S. and Jabbari, F. (2003). "H_2-based control strategies for civil engineering structures," *Journal of Structural Control*, 10(3-4): 205-230.

[16] Zhai, G., Ikeda, M. and Fujisaki, Y. (2001). "Decentralized H_∞ controller design: a matrix inequality approach using a homotopy method," *Automatica*, 37(4): 565-572.